J Mater Sci: Mater Electron (2011) 22:1841–1847
DOI 10.1007/s10854-011-0371-4

Two-step sintering and electrical properties of sol–gel derived $0.94(Bi_{0.5}Na_{0.5})TiO_3$–$0.06BaTiO_3$ lead-free ceramics

Weiqing Meng · Ruzhong Zuo · Shi Su · Xiaohui Wang · Longtu Li

Received: 8 March 2011 / Accepted: 7 April 2011 / Published online: 16 April 2011

Abstract Two-step pressureless sintering of sol–gel derived $0.94(Bi_{0.5}Na_{0.5})TiO_3$–$0.06BaTiO_3$ (BNT-BT) lead-free piezoelectric ceramics were investigated in comparison with conventional sintering. The effect of sintering regimes on the densification, grain growth behavior and electrical properties was discussed in detail. The results indicated that BNT-BT ceramics with a density of 95%, a relatively fine grain size of 850 nm and comparable piezoelectric properties (d_{33} ~170 pC/N, k_p ~0.26, Q_m ~102) had been achieved by pre-sintering at 1,150 °C to reach a critical density of 78%, and then cooling to a lower temperature of 1,050 °C for 20 h. The critical density value proves important at which the grain boundary diffusion could be maintained but the grain boundary migration suppressed at the same time. Moreover, the volatilization loss of Bi and Na elements could be inhibited by two-step sintering. Both the reduction of the grain size and the inhibition of the stoichiometry deviation together account for the variation of various electrical properties.

1 Introduction

The fabrication of fine-grained functional ceramics has become an important research topic in recent years since some special electrical properties can be induced in addition to known effects on mechanical properties. Kinoshita [1] indicated that the dielectric constant of the BT ceramics increased with decreasing the grain size. Karaki [2] reported in the literature when the grain size of the BT ceramics decreased to 1.6 μm, d_{33} ~460pC/N was achieved, which was much larger than coarse grain ceramics. Zou [3] found high piezoelectric property $d_{33} = 520$ pC/N while the grain size of $(1 - x)BiScO_3$–$xPbTiO_3$ were reduced to 200 nm. It can be found the properties of ceramics have been strengthened with decreasing grain size from the above literatures. As an important candidate of lead-free piezoelectric ceramics, $0.94(Bi_{0.5}Na_{0.5})TiO_3$–$0.06BaTiO_3$ near a morphotropic phase boundary has been widely investigated in the past few years. However, nano-sized BNT-BT ceramics usually can not be obtained owing to their high sintering temperature whether the initial power was fabricated by a conventional mixed-oxide or a soft-chemical method [4–7]. Thus, the grain size effect in BNT-BT ceramics has not yet been reported.

Several sintering methods have been used to fabricate nanocrystalline ceramics, such as microwave sintering [8], spark plasma sintering [9], hot press sintering and so on [10], but these methods need special equipments, being sophisticated and expensive for use. The two-step sintering as a pressureless sintering technique has been used to make a couple of nanocrystalline ceramics such as BT [11], Ni–Cu–Zn ferrite [12], ZnO [13], since proposed by Chen and Wang [14]. This sintering method involves the first step of rapidly rising to a high temperature (T_1) to achieve a critical density and follows the second step of rapidly cooling to a relatively low temperature (T_2) with a long holding time (t_2) to ensure enough driving force for grain boundary diffusion to realize a desire final density and while to inhibit the migration of grain

W. Meng · R. Zuo (✉) · S. Su
Institute of Electro Ceramics and Devices, School of Materials Science and Engineering, Hefei University of Technology, 230009 Hefei, People's Republic of China
e-mail: piezolab@hfut.edu.cn

X. Wang · L. Li
State Key Lab of New Ceramics and Fine Processing, Department of Materials Science and Engineering, Tsinghua University, 100084 Beijing, China

boundary for controlling the grain growth. After the first step, all pores should become subcritical and unstable against shrinkage [15]. Residual pores would be filled to promote increased density by grain boundary diffusion only. On the other hand, it was also found that two-step sintering can also benefit to the reduction of sintering temperature as the density can be modulated during the second step through a long-term surface diffusion at a rather low temperature [3, 16, 17]. This should be advantageous for some compositions containing volatile elements such as Na, Pb, K, Bi and so on. The volatilization of Bi and Na in BNT-BT ceramics tends to result in a great deviation from the stoichiometry and the deterioration of electrical properties. It would make sense if the loss of Bi and Na can be minimized by two-step sintering.

According to the literature review, two-step sintering has never been applied to densify BNT-BT lead-free piezoelectric ceramics so far. The purpose of this study is thus to investigate the two-step sintering of BNT-BT ceramics derived by a citrate sol–gel method. The effect of the sintering regimes on the grain growth, densification, microstructure, and electrical properties was systematically discussed.

2 Experimental

Nanoscaled BNT-BT powder used in this study was prepared by a citrate sol–gel method. $NaNO_3$ (≥99.0%), $Bi(NO_3)_3 \bullet 5H_2O$ (≥99.0%), $Ba(NO_3)_2$ (≥99.0%), $Ti(OC_4H_9)_4$ (≥98.0%) were used as starting materials. Citric acid ($C_6H_8O_7 \cdot H_2O$, ≥99.5%) was used as a complexing reagent and ammonia was added to adjust the PH value of the solution. These raw materials were weighed to meet the composition according to the chemical formula. The details of the experimental procedure can be referred elsewhere [18]. The as-prepared gel calcined at 600 °C for 3 h was ball milled for 4 h in ethanol. After drying, the powder was uniaxially pressed into disk samples and sintered by a two-step sintering method as described below: firstly, the samples were heated from room temperature to a high temperature T_1 (1,100–1,200 °C) with a heating rate of 5 °C/min, held for a short time (t_1), and then rapidly decreased to a low temperature of T_2 (950–1,080 °C) at 18 °C/min, and held at T_2 for a long time (t_2). For comparison, some samples were densified by normal sintering, i.e., heating to T_1 with a heating rate of 5 °C/min, and held at T_1 for a certain time (t_1), and then directly cooling to room temperature. In this paper, the symbol "$T_1/t_1/T_2/t_2$" was used to indicate both normal sintering and two-step sintering regimes.

The transmission electron microscope (TEM, Model JEM-2011, JEOL Ltd., Japan) was used to analyze the size and morphology of the as-synthesized powders. The crystal structure of the particle was identified using an X-ray diffractometer (XRD, D/Max-RB, Rigaku, Japan). The data of XRD was also used to estimate the particle size of the powder. The microstructure of the sintered BNT-BT specimens of at different temperatures was observed using a scanning electron microscope (SEM, SSX-550, Shimadzu, Japan). The grain size was estimated by a linear intercept method using SEM photographs on the polished and etched surface of the sintered samples. The density of the specimens was measured by the Archimedes method in distilled water. The pellets were electroded by using silver paste on both surfaces at 550 °C for 30 min. The dielectric constant was measured as a function of temperature by an LCR meter (Agilent E4980A, USA). The piezoelectric constant d_{33} was measured directly on a quasi-static d_{33} meter (YE2730A, Sinocera, China) 24 h after the sample was electrically poled in a silicone oil bath under a dc field of 3 kV/mm at 60 °C for 15 min. The planar electromechanical coupling coefficient k_p, and mechanical quality factor Q_m were determined by a resonance–antiresonance method using a high precision impedance analyzer (PV70A, Beijing Band ERA Co., Ltd. China).

3 Results and discussion

The crystal structure, grain morphology and sintering behavior of BNT-BT powders prepared by a citrate sol–gel method are shown in Fig. 1. It can be seen that pure perovskite structure was obtained after BNT-BT gel was calcined at 600 °C. However, its crystal symmetry looks a cubic, rather than a two-phase coexisted structure of rhombohedral and tetragonal phases [4], probably because of the crystallite size effect. The average crystallite size of the powder was calculated to be ~30 nm from the XRD data (Inset in Fig. 1) by using Scherrer's equation:

$$D = \frac{K\lambda}{\beta \cos\theta} \quad (1)$$

where D is the crystallite size, λ is the X-ray wavelength, θ is the diffraction angle, β is the half-width of the XRD (110) peak, and K is the Scherrer constant. In addition, a direct TEM observation (Inset in Fig. 1) gives an average value ~40 nm of grain size, which approximates to the result by Scherrer's equation. Moreover, it can be observed that there are still some large soft agglomerates in the powder after it was ball milled in ethanol after calcination. The grain size and density of disk samples prepared by uniaxially pressing the as-prepared BNT-BT powder was indicated in Fig. 1 as a function of sintering temperature without holding time ($t_1 = 0$). It can be seen that both grain size and density increase monotonously with increasing

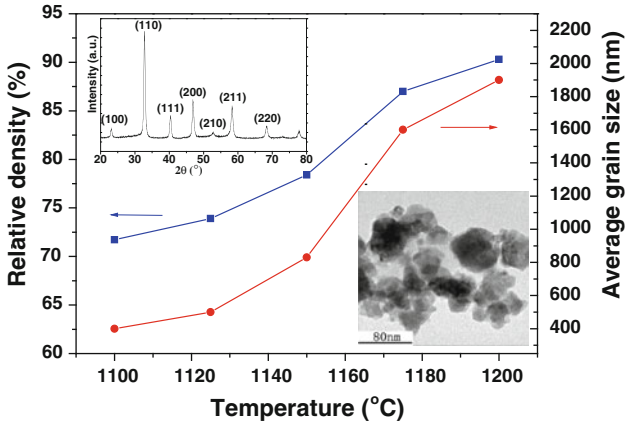

Fig. 1 Densification and grain growth behavior of BNT-BT samples normally sintered in the temperature range of 1,100–1,200 °C without holding time; Insets are the X-ray diffraction pattern and transmission electron micrograph of the sol–gel derived BNT-BT powder calcined at 600 °C for 3 h

temperature. We can see that a relative density of 74% was reached when the temperature was raised to 1,125 °C, which is essentially close to the critical density value (75%) in the literature [15]. Moreover, a big increase in grain size from 830 nm to 1,600 nm happens in the temperature range from 1,150 °C to 1,175 °C (as also can be seen from Fig. 2), probably because the critical density has been reached at the temperature of 1,150 °C such that enough driving force for grain boundary migration tends to cause fast grain growth with further increasing temperature. As the temperature is over 1,175 °C, the increased grain size significantly reduces the intrinsic sintering force of the initial powder but simultaneously increases the distance between the centers of two neighboring grains. Therefore, the grain size and relative density can not increase as rapidly as before.

After the samples underwent the first-step sintering at different temperatures T_1, the effect of sintering temperature T_2 at the second step on the densification and grain growth is indicated in Fig. 3. According to the literature [14], the holding time was setted at 20 h in this part. If T_2 is too low, densification becomes exhausted after the sintering proceeds for a while. However, a high T_2 tends to induce further grain growth. It can be seen that for the first step sintering at $T_1 = 1125$ °C, the final density is still too low (< 95%) although the grain size does not change much as $T_2 \leq 1050$ °C. This means that residual pores were supercritical and thermodynamically stable after pre-sintering at T_1, such that they were hard to be removed. Thus, a relative density of 74% after pre-sintering at 1,125 °C is insufficient for further densification through the second step sintering without obvious grain growth. Mazaheri [13] showed that the value of critical density was 78% for nanocrystalline ZnO. It was also found that the critical density value was 82% for nanocrystalline alumina while it was as high as 92% for submicrometer alumina [19, 20]. There is great difference in the critical density even for the same composition. This proves to be attributed to the grain size and the agglomeration degree of the powder as well as the shaping methods [21]. As T_2 increases to 1,080 °C, the grain grows obviously although the densification is improved as well. We can conclude that both grain boundary diffusion and grain boundary migration occurred in the case.

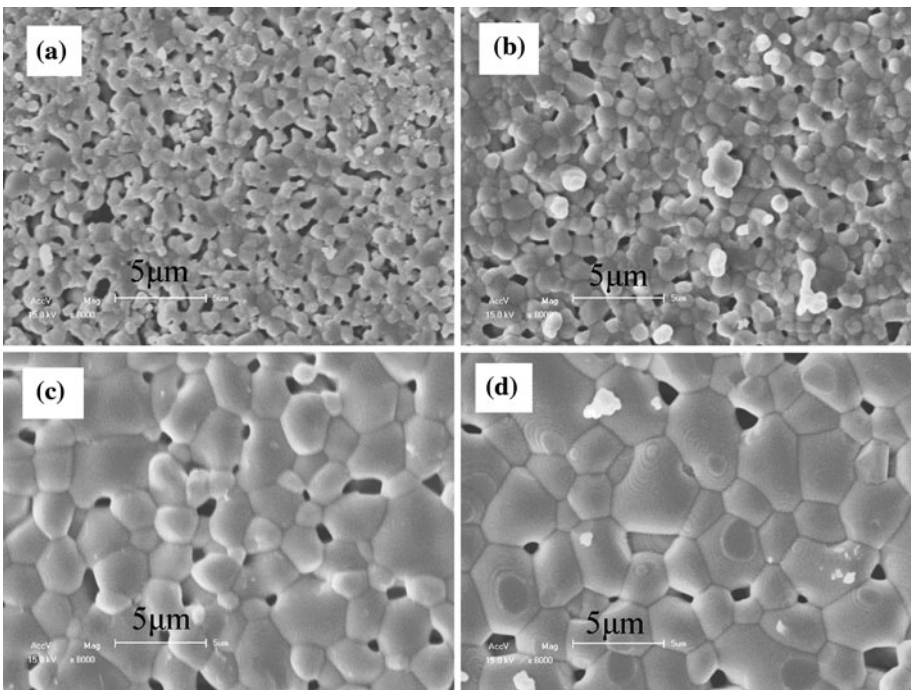

Fig. 2 Scanning electron microscopy photographs of BNT-BT samples normally sintered (t_1=0 h) at (**a**) 1,125 °C, (**b**) 1,150 °C, (**c**) 1,175 °C and (**d**) 1,200 °C

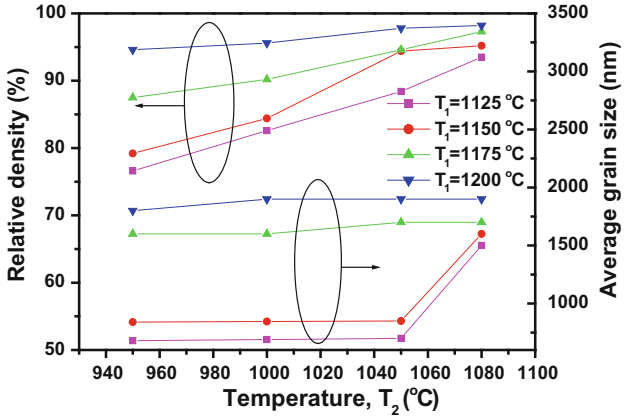

Fig. 3 Densification and grain growth behavior of BNT-BT samples undergoing a two-step sintering regime, T_1/0/T_2/20

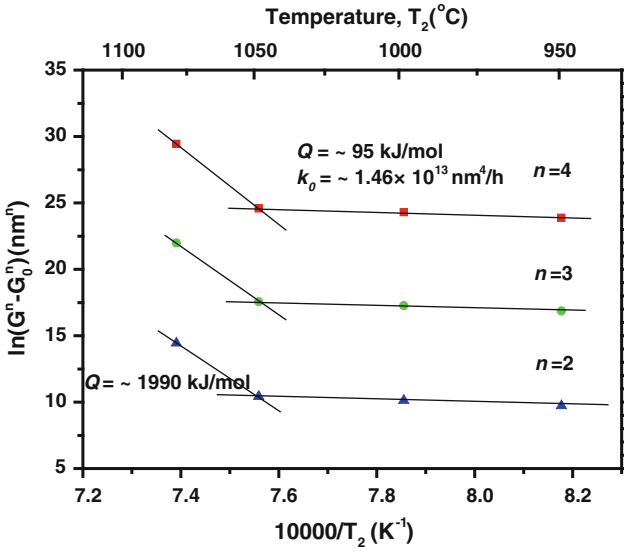

Fig. 4 The plots of $\ln(G^n - G_0^n)$ versus $1/T_2$ for the estimation of activation energy Q

When $T_1 = 1{,}150$ °C (pre-sintered density is 78.4%), no improvement in densification can be seen as $T_2 \leq 1{,}000$ °C, because the densification mechanisms such as grain boundary diffusion and volume diffusion were not active at such low temperatures, such that it is impossible for the matter transportation from the grain boundary to the neck in order to reduce the distance between the centers of the grains, which is usually the main reason for densification [22]. As T_2 is up to 1,050 °C, a relative density of 95% is achieved however there is no significant grain growth (the grain size is 850 nm). It is known that grain growth equation could be generally described as follows [23]:

$$G^{\mathrm{n}} - G_0^n = k_0 t \exp\left(-\frac{Q}{RT}\right) \tag{2}$$

where G is the grain size after the holding time t, G_0 is the grain size after pre-sintering at T_1, n is the grain growth kinetic exponent (when $n = 2$, the grain growth mechanism is grain boundary migration; $n = 3$, the grain growth is controlled by the lattice diffusion mechanism and $n = 4$ for grain boundary diffusion mechanism) [24, 25], k_0 is a constant, Q is the activation energy for the grain growth process, R is the gas constant, and T is the sintering temperature. For the case of samples sintered at different $T = T_2$ for $t = t_2 = 20$ h after pre-sintering at 1,150 °C. Equation (2) can be rewritten as follows by logarithmizing the two sides:

$$\ln\left(G^n - G_0^n\right) = -\frac{Q}{R} \cdot \frac{1}{T_2} + \ln k_0 + \ln t_2 \tag{3}$$

from which Q value could be calculated from the slopes of $\ln(G^n - G_0^n)$ versus $1/T_2$ curves as shown in Fig. 4. It can be seen that the data can not be simply fitted with a straight line no matter what the n value is. Each curve can be divided into two sections corresponding to different slopes. The part with a small slope for $n = 4$ could be attributed to a dominant mechanism (grain boundary diffusion). On the contrary, another part with a large slope could be assigned to the grain boundary migration mechanism although limited number of date points in this part may cause some errors for the prediction. Thus, the activation energies Q of the grain boundary diffusion and grain boundary migration mechanism could be estimated to be ~95 kJ/mol and ~1990 kJ/mol, respectively. The constant k_0 for the grain boundary diffusion mechanism could be calculated to be $\sim 1.46 \times 10^{13}$ nm^4/h. It is evident that the activation energy for the grain boundary migration is much more higher than that of the grain boundary diffusion. Therefore, in this case the driving force should be enough to maintain the grain boundary diffusion for further increasing the density, while insufficient for the grain boundary migration. In other words, it was shown that a relative density of 78.4% might have reached the critical density of the studied samples.

Moreover, it can be seen from Fig. 2 that the grain size has become quite large only after the first step at $T_1 \geq 1175$ °C. More energy is thus required for grain boundary migration in this case [14, 26], because the driving force of intrinsic surface diffusion decreases with increasing the grain size. Therefore, compared to the case that samples were sintered at 1125/0/1080/20 and 1150/0/1080/20 regimes, grains did not grow any more for sintering regimes of 1175/0/1080/20 and 1200/0/1080/20. Although nanocrystalline ceramics can not be obtained in those cases, yet the sintering temperature was obviously decreased, for example, the density can be larger than 95% for 1200/0/950/20. Both nearly zero holding time at high temperature T_1 and very low temperature T_2 even for a long

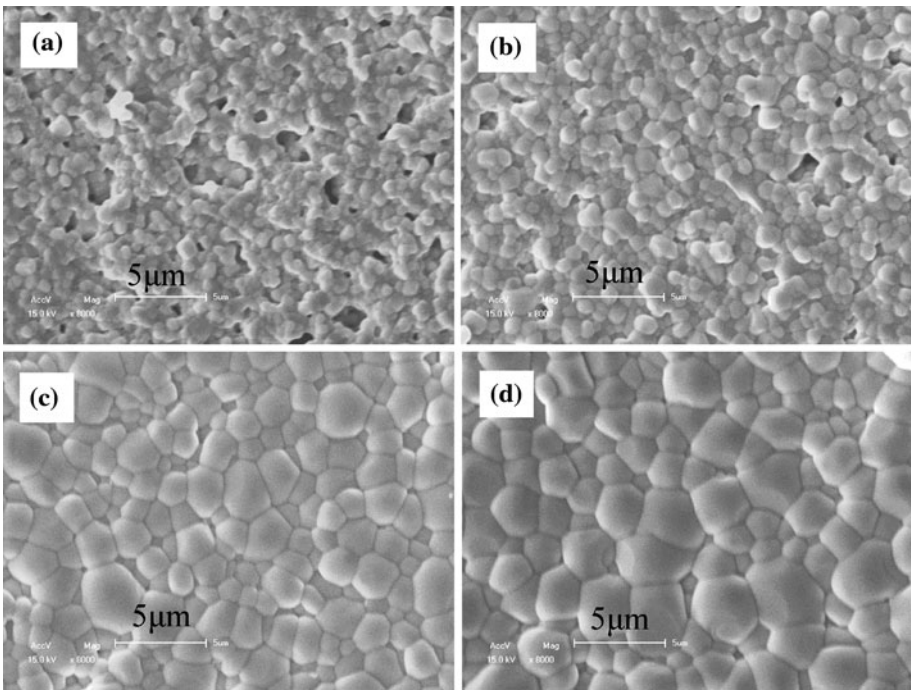

Fig. 5 Scanning electron microscopy photographs of BNT-BT samples after a two-step sintering, T_1/0/1050/20: (**a**) T_1 = 1,125 °C, (**b**) T_1 = 1,150 °C, (**c**) T_1 = 1,175 °C and (**d**) T_1 = 1,200 °C

holding time may significantly help inhibit the volatilization loss of Bi and Na elements in BNT-BT ceramics. The grain morphology of BNT-BT samples sintered at T_1/0/1050/20 regimes is compared in Fig. 5. For T_1 = 1,125 °C, a large number of pores left in the sample, resulting in insufficient densification. For T_1 = 1,150 °C,a desired densification was reached, accompanied by a relatively fine grain size (850 nm), compared to that of normally sintered samples (1,300 nm at 1140/3/0/0) as shown in Table 1.

For the case of T_1 = 1125 °C, the pre-sintered density (74%) is insufficient, making the pores subcritical and unstable, such that pores can not effectively be removed by grain boundary diffusion even if holding time is prolonged for 40 h. However, the surface diffusion is active at this moment, which contributes the grain growth without any effect on densification [13]. For T_1 = 1,150 °C, residual pores become critical, acting as pinning agents of grain boundary migration [15, 27, 28]. Therefore, the grain size remains almost constant during t_2 = 0–20 h, although the relative density increases obviously, as shown in Fig. 6. For samples sintered at T_2 = 1,050 °C for different t_2 after pre-sintering at 1,150 °C, Eq (2) can be rewritten as follows:

$$\ln\left(G^n - G_0^n\right) = \ln t_2 + \ln k_0 - \frac{Q}{R}\cdot\frac{1}{T_2} \tag{4}$$

according to which a straight line with a slope of 1.0 could be drawn if we plot $\ln(G^n - G_0^n)$ as a function of $\ln t_2$ (n = 4, assuming that grain growth was controlled by the grain boundary diffusion mechanism). As shown in Fig. 7, these

Table 1 Sintering Behavior and Various Electrical Properties of BNT-BT Samples under Different Sintering Regimes

Sintering regimes ($T_1/t_1/T_2/t_2$)		Relative density (%)		Grain size (nm)		d_{33} (pC/N)	k_p	Q_m	T_d (°C)
		After T_1	After T_2	After T_1	After T_2				
Normal sintering	1140/3/0/0	95.0	–	1300	–	168	0.32	128	135
	1160/3/0/0	97.3	–	1300	–	173	0.33	119	140
	1180/3/0/0	96.1	–	1800	–	168	0.32	121	144
Two-step sintering	1125/0/1080/20	73.9	93.5	700	1500	158	0.27	158	118
	1150/0/1050/20	78.4	95.0	830	850	170	0.26	102	116
	1150/0/1050/40	78.4	96.9	830	1000	171	0.33	125	118
	1175/0/1050/20	87.0	95.2	1600	1700	172	0.32	123	126
	1200/0/950/20	90.3	95.1	1900	1900	176	0.29	102	120
	1200/0/1000/20	90.3	95.6	1900	1900	176	0.29	109	124

BNT-BT: $0.94(Bi_{0.5}Na_{0.5})TiO_3$–$0.06BaTiO_3$

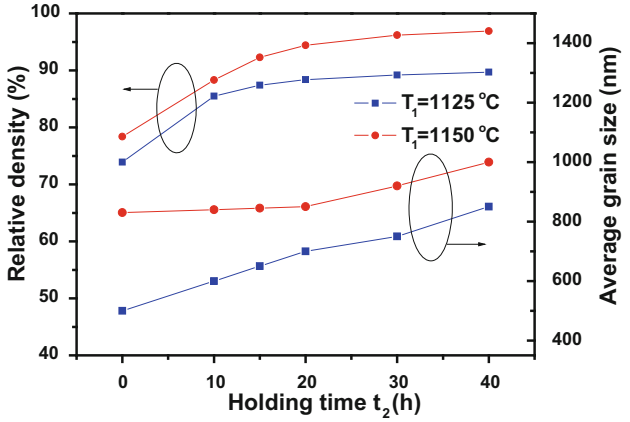

Fig. 6 Densification and grain growth behavior of BNT-BT samples after two-step sintering regimes, T_1/0/1050/t_2

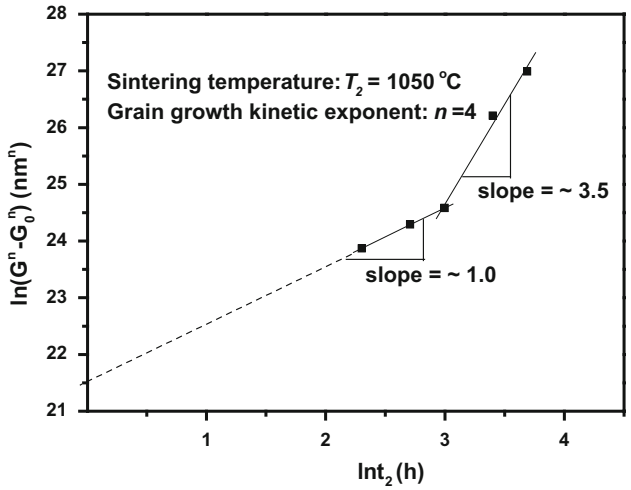

Fig. 7 The plot of $\ln(G^n–G_0^n)$ versus $\ln t_2$ ($n = 4$, assuming that grain growth was controlled by the grain boundary diffusion mechanism)

date points were well fitted when the holding time $t_2 \leq 20$ h. By extrapolation method, the activation energy Q of ~99 kJ/mol was achieved, which approximates to the calculation from Fig. 4, meaning that the grain boundary diffusion still played a dominant role. But the slope increased to ~3.5 when $t_2 > 20$ h, indicating that the grain growth mechanism has changed. It is reasonable that the number of open pores decreases with further increasing the density of the samples (with increasing holding time t_2). The pinning effect of pores then tends to be wasted such that the grain boundary migration can not be inhibited, resulting in accelerated grain growth. Therefore, the holding time t_2 of 20 h should be appropriate for getting an accepted density without significant grain growth.

The dielectric constant of BNT-BT ceramics sintered under different regimes is plotted as a function of

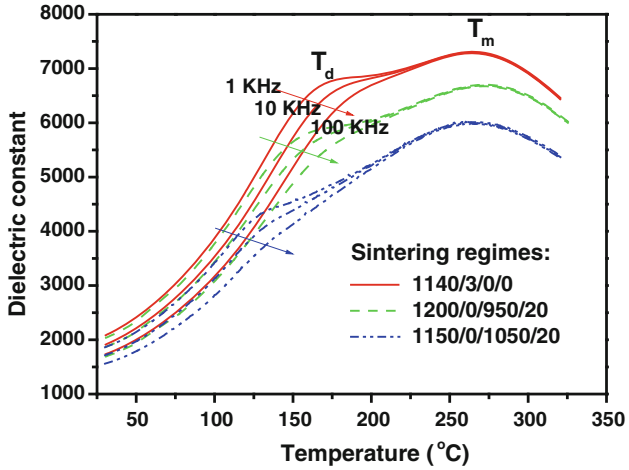

Fig. 8 Dielectric constant as a function of measuring temperature and frequency of BNT-BT ceramics sintered under different regimes as indicated

measuring temperature and frequency, as shown in Fig. 8. Note that all three samples have close sintered density of ~95%. It can be seen that the temperatures at phase transition and the dielectric constant values vary owing to different regimes. Compared to normal sintering (1140/3/0/0), two-step sintering tends to cause relatively decreased dielectric constant value and lower ferroelectric-antiferroelectric phase transition temperature (T_d). The temperature where the dielectric constant reaches the maximum (T_m) seems insensitive to the sintering regimes. Moreover, BNT-BT samples densified under 1150/0/1050/20 exhibit a more diffuse phase transition at T_d and a lower dielectric constant than those under the other two regimes. The piezoelectric, electromechanical properties as well as the depolarization temperature T_d of BNT-BT ceramics through different sintering regimes are also listed in Table 1. On the one hand, one can see that BNT-BT ceramics through two-step sintering of 1150/0/1050/20 own a desired density of 95% and a relatively fine grain size of 850 nm and comparable piezoelectric and electromechanical properties ($d_{33} = 170$ pC/N, $k_p = 0.26$ and $Q_m = 102$) to those of conventionally sintered samples. At the same density (for example 95%), normally sintered samples have an average grain size of 1,300 nm. Although the density of 90° ferroelectric domain per volume may increases as the grain size is reduced [29], yet this positive effect on piezoelectric properties could be counteracted by a negative effect from increased grain boundary effect occurred in a fine-grain sample. The fine grain size could be also responsible for the increased diffusivity of phase transition at T_d. On the other hand, the volatile elements such as Bi and Na could become easier to loss for normal sintering regimes (for example, 1140/3/0/0) than two-step sintering regimes (for example, 1200/0/950/20), meaning

that the amount of TiO_2 is excessive, which could suppress the occurrence of phase transition from rhombohedral ferroelectric to tetragonal antiferroelectric phases [30]. This may be the reason why the depolarization temperatures T_d obtained for normal sintering were moved to higher temperatures. That is to say, compared to normal sintering, the reduced loss of volatile elements for two-step sintering might weaken the compositional deviation from the stoichiometry.

4 Conclusions

BNT-BT lead-free ceramics derived from a citrate sol–gel method were densified by normal sintering and two-step sintering, respectively. The critical density value of $\sim$78% was achieved after samples were pre-sintered at 1,150 °C such that a relatively fine grain size of 850 nm and comparable piezoelectric properties ($d_{33} = 170$ pC/N, $k_p \sim 0.26$ and $Q_m = 102$) were obtained through a second-step sintering at 1,050 °C for 20 h. Residual pores under a critical state after pre-sintering (1,150 °C) could pin the grain boundary migration and further densification was realized by the grain boundary diffusion activated by choosing an appropriate sintering temperature T_2 (1,050 °C). Compared to the normal sintering, two-step sintering technique could also effectively decrease the sintering temperature of BNT-BT ceramics, which could help alleviate the volatilization loss of Na and Bi elements at a high sintering temperature.

Acknowledgments This work was financially supported by joint project of Chang-Shan-Jiao of Anhui Province (10140702014), a project of Natural Science Foundation of Anhui Province (090414179), by the Fundamental Research Funds for the Central Universities, and by the National Natural Science Foundation of China (50972035) and a Program for New Century Excellent Talents in University, State Education Ministry (NCET-08-0766) and 973 Program (No. 2009CB623301).

References

1. K. Kinoshita, A. Yamaji, J. Appl. Phys. **47**, 371 (1976)
2. T. Karaki, K. Yan, M. Adachi, Jpn. J. Appl. Phys. **46**, 7035 (2007)
3. T.T. Zou, X.H. Wang, W. Zhao, L.T. Li, J. Am. Ceram. Soc. **91**, 121 (2008)
4. T. Takenaka, K. Maruyama, K. Sakata, Jpn. J. Appl. Phys. **30**, 2236 (1991)
5. B.J. Chu, D.R. Chen, G.R. Li, Q.R. Yin, J. Eur. Ceram. Soc. **22**, 2115 (2002)
6. H.Q. Wang, R.Z. Zuo, X. Ji, Z.K. Xu, Mater. Des. **31**, 4403 (2010)
7. J.G. Hou, Y.F. Qu, W.B. Ma, D. Shan, J. Mater. Sci. **42**, 6787 (2007)
8. H. Takahashi, Y. Numamoto, J. Tani, S. Tsurekawa, Jpn. J. Appl. Phys. **45**, 7405 (2006)
9. J.M. Wang, L. Gao, J. Am. Ceram. Soc. **88**, 1637 (2005)
10. A. Weibel, R. Bouchet, R. Denoyel, P. Knauth, J. Eur. Ceram. Soc. **27**, 2641 (2007)
11. X.H. Wang, X.Y. Deng, H. Zhou, L.T. Li, I.W. Chen, J. Electroceram. **21**, 230 (2008)
12. X.H. Wang, X.Y. Deng, H.L. Bai, H. Zhou, W.G. Qu, L.T. Li, I.W. Chen, J. Am. Ceram. Soc. **89**, 438 (2006)
13. M. Mazaheri, A.M. Zahedi, S. Sadrnezhaad, J. Am. Ceram. Soc. **91**, 56 (2008)
14. I.W. Chen, X.H. Wang, Nature **404**, 168 (2000)
15. X.H. Wang, P.L. Chen, I.W. Chen, J. Am. Ceram. Soc. **89**, 431 (2006)
16. J. Fang, X.H. Wang, Z.B. Tian, C.F. Zhong, L.T. Li, R.Z. Zuo, J. Am. Ceram. Soc. **93**, 3552 (2010)
17. D.L. Wang, K.J. Zhu, H.L. Ji, J.H. Qiu, Ferroelectrics **392**, 120 (2009)
18. H.Q. Wang, R.Z. Zuo, Y. Liu, J. Fu, J. Mater. Sci. **45**, 3677 (2010)
19. K. Bodišová, P. šajgalík, D. Galusek, P. švančárek, J. Am. Ceram. Soc. **90**, 330 (2007)
20. Z. Razavi Hesabi, M. Haghighatzadeh, M. Mazaheri, D. Galusek, S. Sadrnezhaad, J. Eur. Ceram. Soc. **29**, 1371 (2009)
21. P. Bowen, C. Carry, Powder Technol. **128**, 248 (2002)
22. M. Fathi, M. Kharaziha, Mater. Lett. **63**, 1455 (2009)
23. R.J. Brook, in *Ceramic Fabrication Processes*, ed. by F.F.Y. Wang (Academic Press, New York, 1976), p. 331
24. L. Lu, N.R. Tao, L.B. Wang, B.Z. Ding, K. Lu, J. Appl. Phys. **89**, 6408 (2001)
25. F. Gao, R.Z. Hong, J.J. Liu, Y.H. Yao, C.S. Tian, J Electroceram. **24**, 145 (2010)
26. C.J. Wang, C.Y. Huang, Y.C. Wu, Ceram. Int. **35**, 1467 (2009)
27. M. Mazaheri, A. Simchi, F. Golestani-Fard, J. Eur. Ceram. Soc. **28**, 2933 (2008)
28. K. Maca, V. Pouchly, Z. Shen, Integr. Ferroelectr. **99**, 114 (2008)
29. G. Arlt, D. Hennings, J. Appl. Phys. **58**, 1619 (1985)
30. X.X. Wang, S.W. Or, X.G. Tang, H.L.W. Chan, P.K. Choy, P.C.K. Liu, Solid State Commun. **134**, 659 (2005)